

## Chapter 2

# Practical Productions of Graphene, Supply and Cost

Graphene in small platelets of high aspect ratio is available by chemical exfoliation of graphite, with a variety of methods and a long history. Graphite is a widely available mineral, at a cost between \$1.50 and \$2.00 per kg, according to “Mineral Commodity Summaries 2013” published by US Department of the Interior and US Geological Survey. (For comparison, the same source estimates indium metal at ~\$650 /kg, with a separate estimate for indium tin oxide, ITO, that is deposited on glass to make the leading form of transparent conductor, as \$800 /kg.) Typically, however, the exfoliation processes leave nano-platelets of only 100–500 nm lateral extent, single monolayer to tens of monolayers in thickness, with defects primarily, but not entirely, at the edges. A contemporary example is “Graphene Nanoplatelets, Grade C” sold by XG Sciences, of Lansing MI, USA. This product, that can be specified at surface area 300, 500 or 750 m<sup>2</sup>/g, is described as “aggregates of sub-micron platelets that have a particle diameter less than 2 microns and particle thickness of a few nanometers, depending on the surface area”. The XG Sciences data sheet, available at <http://xgsciences.com/products/graphene-nanoplatelets/grade-c/>, indicates a substantial impurity level, 10 % by weight of oxygen, with the comment “Nanoplatelets have naturally occurring functional groups like ethers, carbonyls, or hydroxyls...present on the edges of the particles and their wt % varies with particle size.” This may be expected in any graphene platelet, since unfilled trigonal carbon bonds at the edges will easily react with ambient gas. This may not be serious, because the impurity will be weakly held and probably can be driven off with annealing, perhaps followed hydrogen annealing to fill the bonds, at the end of processing. While a price list is not available, Samba Sivudu and Mahajan (2012) suggest a cost in excess of \$220 /kg for a similar XG Sciences product. (For comparison, Norit GSX, an “activated carbon” characterized by surface area about 950 m<sup>2</sup>/g, with curved rather than flat morphology, and possessing lateral planar extents less than 20 nm, is offered by Alfa Aesar at \$290 for 2 kg. Such “activated charcoal” products are sold in large volume for water purification.) To make a coherent electrical conductor, platelets such as offered by XG Sciences must be deposited, typically by spinning, to produce a layer whose conductivity depends on the contact between the overlapping individual grains, that are too refractory to sinter. Other important forms of small particle carbon come from heating

petroleum, coal, peat, coconut shells, or chemicals such as polyacrylonitrile (PAN, rayon) in the absence of oxygen. These typically are large volume, low cost, processes. One practical distinction between exfoliated graphene platelets and the other forms of particulate carbon is the large aspect ratio of the platelets.

Centimeter- and even meter- scale sheets of monolayer graphene are a recent development, presently largely a laboratory phenomenon, but clearly destined for electronic applications. The primary source of large sheets of monolayer graphene is by chemical vapor deposition of a hydrocarbon such as methane (or benzene) onto a hot Cu or Ni surface. A second source is by heating single crystals of SiC such that Si sublimates and C precipitates as graphene in an epitaxial fashion. In the first case the copper substrate is usually not useful and is removed by its chemical dissolution. As mentioned earlier, Bae et al. (2010) have achieved polycrystals of lateral extent one meter by such a method, finding a practical approach to removing the copper substrate. That this is not an inexpensive process is suggested by the selling price (Graphene Square, Seoul, South Korea) of \$264 for a single  $50 \times 50$  mm sheet of monolayer graphene on copper foil.

## 2.1 Graphite-Based Methods

Graphene, in multi-layer, nano-platelet forms, has long been available inexpensively by chemical “exfoliation” treatments of graphite, a mineral found in the earth. These forms are generally used as additives to composites, bringing electrical conductivity and mechanical flexibility and strength. It is unclear at the moment whether such graphite-based materials will be of sufficiently high conductivity, when formed into electrodes, to suffice in applications such as solar cells or interconnects in chip manufacture. An assessment of production of higher quality exfoliated graphene, on the scale of tons per year, was given by Segal (2009). A recent excellent survey of the whole spectrum of graphene applications has been given by Novoselov et al. (2012), who are able to project costs for the various types of graphene and to predict where opportunities for market penetration will appear.

The chemical exfoliation of graphite, first reported by Brodie (1859) and Staudenmaier (1898), proceeds by treating graphite with acid leading to graphite oxide flakes (originally called “graphon”). Graphite oxide is an insulating layer compound with interplane spacing approximately 0.65–0.75 nm. According to Novoselov (2011), graphite oxide can be regarded as graphite intercalated with oxygen and hydroxyl groups, thus a hydrophilic material easily dispersed in water. Such a dispersion includes extremely thin, even monolayer, oxide flakes that can be subsequently reduced, e.g., using hydrazine, according to Ruess and Vogt (1948) and Hummers et al. (1958), or by rapid heating in inert gas (Schniepp et al. 2006) to pure carbon. Such samples, as mentioned, are now regarded as low-quality graphene, although it is clear that the low cost may place them in applications. A suggested structure for Graphite Oxide, with prominent  $sp^3$  bonding of

carbon and oxygen atoms (due to Jo et al. 2012) is shown in Fig. 2.1. This Figure also schematically shows the reduced defective graphene obtained with hydrazine treatment. Quoting Mkhoyan et al. (2009), “the graphite oxide is rough, with an average surface roughness 0.6 nm and the structure is predominantly amorphous due to distortions from  $sp^3$  C–O bonds. Around 40 %  $sp^3$  (tetrahedral) bonding was found..”. The nature of the “low quality graphene” following reduction of graphite oxide was also characterized in a careful and extensive study of Schniepp et al. (2006).

In their experimental work, Schniepp et al. start with graphite flakes that are reacted in an oxidizing solution of sulfuric acid, nitric acid, and potassium chlorate (similar to the above-cited process of 1898). Schniepp et al. (2006) find that 96 h in the oxidizing solution is needed to completely remove, in x-ray examination, the 0.34 nm interplanar spacing characteristic of graphite, to supplant that spacing with a 0.65–0.75 nm spacing characteristic of graphite oxide in its solid phase. The treatment is likely to form OH hydroxyl, C–O–C epoxide and COOH (O=C–OH) carboxyl groups, mostly near defect sites. The following thermal exfoliation of the solid graphite oxide flakes is akin to an explosion releasing  $CO_2$  gas. This is accomplished by placing a sample of completely dried solid-phase graphite oxide, in a quartz tube purged with argon gas, into a furnace preheated to 1,050 °C. The rapid (>2,000 °C/min) heating splits the graphite into single sheets through the evolution of  $CO_2$  gas. Atomic Force microscopy was among the methods used to establish the single layer nature of the resulting graphene particles, whose lateral dimension is typically 200–500 nm. This careful modern study of the early (Brodie 1859) inexpensive, bulk chemical exfoliation process, and its several variations, concludes that single-layer graphene can (but rarely does) result from such processes, but that any such graphene retains in-plane defects, mainly structural defects, such as kinks and 5-8-5 defects remnant of the successive oxidizing and reduction reactions. (A 5-8-5 defect replaces three 6-membered rings with rings containing 5 and 8 bonds.) In addition one finds remnant chemical impurities like C–O–C (epoxy) or C–OH groups (within the graphene planes) and C–OH and –COOH groups at the edges. The defects clearly remain in the basal plane of the final graphene, as well as at its edges. The defects may have a useful functionalizing role in an additive to a composite material, but are definitely undesirable in graphene intended as a conductive electronic component. Schniepp et al. (2006) measure the electrical conductivity of compacts of their powdered material in the range 1,000–2,300 S/m (0.043–0.1  $\Omega$ -cm). These resistivities, somewhat smaller than for other small-particle carbon products, are probably still dominated by the nature of interparticle contacts.

A device-oriented study of nanoribbons produced by chemical exfoliation is that of Li et al. (2008). These authors find chemical means of producing narrow nanoribbons with smooth boundaries starting with graphite oxide, and go on to closely characterize the nanoribbons by electrical methods. The method of Li et al. (2008) is based on a commercial product, “expandable graphite” (Grafguard 160-50 N, Graftech Incorporated, Cleveland, OH). It appears that this material is graphite oxide, since it is readily expanded by heating, as Li et al. (2008) have

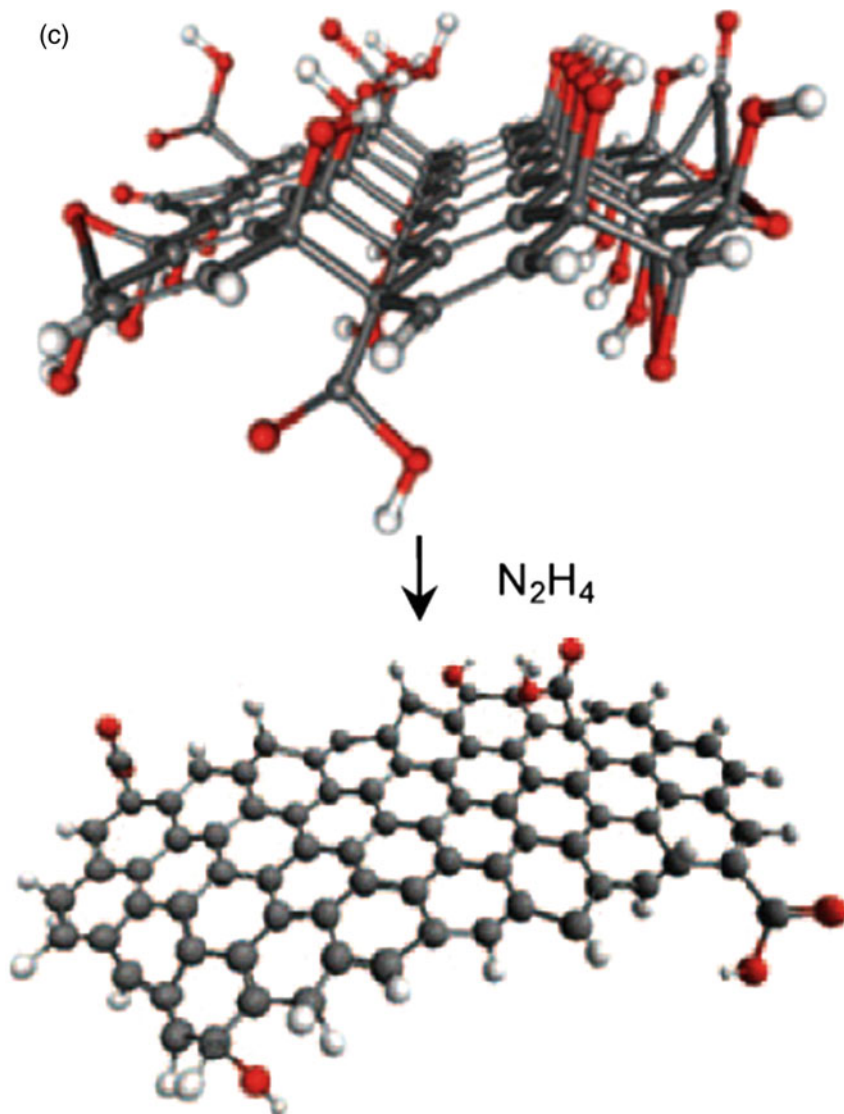


**Fig. 2.1** Schematic diagram of reduction (using hydrazine  $N_2H_4$ ) of graphite oxide to graphene with retained defects. *Open symbols* are hydrogen, others are carbon and oxygen. (Jo et al. 2012, Fig. 2c) (Reprinted figure with permission from Tung et al., Fig. 1. Copyright (2009) by the Nature Nanotechnology)

done. The “expandable graphite” is exfoliated by heating for 60 s at 1,000 °C in forming gas (3 % hydrogen in argon). Volatile gaseous species violently form from the intercalants, and exfoliate the material into a loose stack of few-layered

graphene sheets. The thermal exfoliation step is critical and responsible for the formation of one- to few-layer graphene, and was revealed to Li et al. (2008) by a volume expansion by  $\sim 100\text{--}200$  times after exfoliation.

The resulting exfoliated graphite was dispersed in a 1,2-dichloroethane (DCE) solution of poly(m-phenylenevinylene-co-2,5-dioctoxy-p-phenylenevinylene) (PmPV), by sonication for about 30 min to form a homogeneous suspension. (Centrifugation then removed large pieces and the remaining suspension was surveyed for its content of planes and ribbons of graphene.) The PmPV polymer non-covalently functionalizes the exfoliated graphene, leading to a homogeneous black suspension during the sonication process. The authors note that the PmPV was necessary to reach a stable suspension. It appears that the polymer adheres to graphene by van der Waals forces similar in magnitude to the binding force of graphene in graphite itself, and that otherwise graphene will not disperse even in the organic solvent.

Li et al. (2008) found that the sonication time to produce ribbons should be optimized, since ribbons were no longer found after hours of sonication. Extended sonication evidently breaks up ribbons and leads to ever-smaller particles. In general, the GNR (graphene nano ribbon) content was smaller than that of sheets: the solution after centrifugation contains micrometer-sized graphene sheets and nanoribbons. The survey of the solution products was carried out using atomic force microscopy (AFM), after removing the PmPV by calcining at  $400\text{ }^{\circ}\text{C}$ . Particular interest was in finding nanoribbons in the sonicated solution products, that were tested by forming a device geometry. Thus, the nanoribbons, harvested from the sonicated suspension as described above, were built into field-effect transistor-like structures, choosing ribbons with widths  $W$  in the range  $10\text{--}55$  nm. These ribbons were placed on an oxidized  $p^{++}$  Si wafer, that formed the back-gate of the field-effect transistor (FET). Palladium Pd contacts were attached to the nanoribbons, to act as source and drain. The devices were surveyed as to the On/Off current ratios, that were found to rise dramatically at small nanoribbon widths  $W$ , less than 10 nm. More details on similar devices regarded as sub-10 nm graphene nanoribbon GNR field-effect transistors were given by Wang et al. (2008). The study indicated that an energy gap dependent on ribbon width is a reliable feature. Although these ribbons must have defects in the graphene planes as a consequence of the chemical oxidation/reduction sequence employed, the main impediment to their use in electronics is similar to that of carbon nanotubes, regarding the difficulty in placing many similar elements in exact locations on a chip.

A proprietary chemical approach leads to the well-known commercial product Grafoil, where graphite oxide is reduced back to pure carbon in thicknesses of hundreds of layers. Grafoil is in the form of a cloth used for sealing joints at high temperature and as a moderator of high energy neutrons in nuclear reactors, because of the low mass of the carbon atom. In the paper of Schiffer et al. (1993), the surface area of Grafoil was measured to be  $33.3\text{ m}^2$  for 2.55 g. (The surface area of fully exfoliated graphite is much larger, namely  $2,630\text{ m}^2/\text{g}$ ) This surface area suggests sheet thickness of hundreds of graphene layers. The “Grafoil GTA

Premium Flexible Graphite” sheet has a density of 1.12 g/cc (compared with 2.27 g/cc for single crystal graphite). It is available in a variety of thicknesses.

For the higher quality electronic applications that may include solar cell electrodes and chip interconnects, variants on the exfoliation process that lead to higher electrical conductivity, but still low cost, are needed. The basic difficulty is that graphite flakes are hydrophobic and will not disperse in water under sonication, and the chemical method of oxidation followed by reduction leads to graphene planes with many defects and lower inherent conductivity.

We mention three alternative approaches to exfoliation of graphite, avoiding the acid oxidation followed by reduction. These are: intercalation with alkali metals, direct exfoliation by sonication in organic solvents, and a process called “edge-carboxylation”. In these processes, no damage is done to the inner portions of the graphene planes, and the exfoliation occurs from the edges of the graphite flakes without oxidation of the graphene planes.

In the intercalation-based exfoliation method of Shioyama (2001) the graphite was first intercalated with potassium, by heating in the presence of K vapor, at a temperature as low as 200 °C. This leads to electron doping of the graphene, and stoichiometric intercalation phases of graphite are well known (Dresselhaus and Dresselhaus 1981).

Shioyama found that heating the resulting K-Graphite Intercalation Compound (KC<sub>8</sub>) at room temperature in a pressure 67 kPa of the vapor 1,3-butadiene (with similar results for the vapor of styrene) led to an exfoliation reaction, evident by the expansion of the K-GIC along its c-axis. The reaction proceeded until all the butadiene vapor was used up. Shioyama suggested that linear polymers were growing, forcing the graphite planes apart. Heating the resulting black elastic polymer above 400 °C resulted in complete release of the potassium polymers, leaving a residue of pure graphitic carbon, completely exfoliated. This process leaves the graphene planes intact with high electrical conductivity. The refractory and inert nature of graphene aids in this process, but high temperature processes are often difficult and expensive from a production viewpoint.

Classes of organic solvents can disperse graphite flakes under sonication. Liquid phase exfoliation without the oxidation/reduction steps used by Schniepp et al. (2006), and earlier workers (thus, strictly speaking, not a *chemical* exfoliation, but by directly dispersing graphite in other, mostly organic, solvents), has been discussed by Hernandez et al. (2008). Their method starts with powdered graphite and leads to dispersions of graphene in the solvent at concentrations up to 0.01 mg/ml. In the case of solvent NMP (N-methylpyrrolidone) a plot of the thickness of the dispersed flakes peaks at about two layers per sheet, using electron microscopy on the resulting particles. The authors have compared results with results from three additional organic solvents. They present their scalable method as potentially useful for large area applications from device and sensor fabrication to conductive composites.

A second example of direct liquid phase exfoliation to produce single layer graphene sheets is described by Mao et al. (2011). In this paper, see references therein, graphene is prepared by liquid phase exfoliation by direct sonication of

graphite in the organic solvent, N-methyl-pyrrolidone (NMP). In more detail, graphite flakes with a size of 1.8–5 mm (from NGS Naturgraphit GmbH, Leinburg, Germany) were incubated in 1 mL N-methyl-pyrrolidone in a 1.5 mL glass vial and sonicated for 3 h. The sonicated solution was then centrifuged at 500 rpm for 90 min. Individual graphene sheets were put onto a grid for examination in a transmission electron microscope (TEM).

It appears that exfoliation of graphite can be initiated at the edges of platelets, leaving fewer in-plane defects. A recent approach employs ball-milling of graphite with dry ice, to produce edge-carboxylated graphite (ECG) nanosheets, of size 100–500 nm, as described by Jeon et al. (2012). The resulting graphene platelets are superior to those obtained by chemical exfoliation because the interior hexagonal planes are undisturbed by the processing. The process breaks up the graphite from the edges, leaving flat hexagonal lattice planes, without the wrinkles and in-plane defects that were noted as a result of chemical exfoliation. The carboxylated edges make the ball-milled product directly dispersible in water and other polar solvents, in the form of individual planes. The carboxylated edges can later be removed by heating, e.g., after a dispersion has been deposited on the target surface. It is suggested that optically transparent films of superior conductivity can be achieved after depositing such nanosheets on surfaces, including silicon, followed by heating. It appears that this process may be inexpensive in bulk production, and that it may further the application of graphene intended as low cost electrodes. Some aspects of the ECG process are illustrated in Fig. 2.2.

The left-most image in Fig. 2.2, above, suggests that “Edge-Carboxylated Graphite” (ECG) can be reversibly obtained from graphite (center) by the ball milling procedure in dry ice. The ECG retains undefected hexagonal basal planes in platelets of size 100–500 nm, and can be reversed to pure graphite by direct annealing. In contrast (on the right) the basic chemical exfoliation route oxidizes the plane surfaces as well as the edges (a suggested structure for GO was shown in Fig. 2.1), and cannot be reversed to pure graphite by direct annealing. As mentioned earlier, when explosive exfoliation is applied to GO, reducing it to graphene, defects remain in the planes. According to Schniepp et al. (2006), to obtain single layers of GO the acid processing of graphite flakes had to last 96 h. Presumably in most cases the acid processing is of shorter duration and commonly leaves multilayers of graphite, and these multilayers are preserved in the explosive heating process. Multilayers of graphite have applications, presumably the Grafoil product is of this type. Electronic applications are more likely to require monolayer- to few-layer un-defected graphite, as is claimed to result from the ball milling process of Jeon et al. (2012).

See also, for the development of the various chemical methods, works of Stankovich et al. (2005), (2006); Dikin et al. (2007); Gomez-Navarro et al. (2007); Ruoff (2008); and Park and Ruoff (2009).

All of the above solution-based methods, chemical or liquid or edge-carboxylated exfoliations, lead to dispersions of very small 200–500 nm graphene flakes with thicknesses one to several monolayers, in units of 0.34 nm. To make a transparent conducting electrode, the tiny flakes are deposited on a substrate, typically by

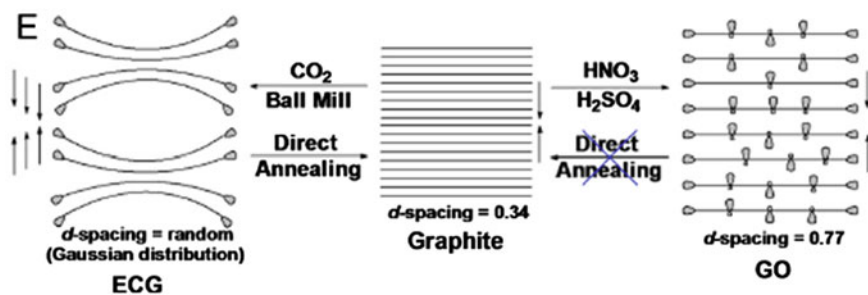


**Fig. 2.2** Schematic comparison of graphite (*center*), with “edge-carboxylated graphite” (ECG) (*left*), and graphite oxide (GO) (*right*). (Reprinted figure with permission from Jeon et al., Fig. 3e. Copyright (2012) by the Proceedings of the National Academy of Sciences)

spin-coating, and the solvent driven off by heating. The resulting conductor is comprised of partially overlapping stacked graphene flakes, with little end-to-end contact, and thus exhibits significant flake-to-flake resistance. The conductivity in the normal direction that is needed for current flow in the stacked deposit is less than the c-axis conductivity in graphite, where the graphene layers are in accurate Bernal stacking, not present in the spin-coated product. The inherent weakness of electrical contact among the deposited platelets is a feature approximately independent of the in-plane defect density of the individual platelets, and stands to reduce the advantage of the less-violent exfoliation methods in the conductivity of the resulting electrode.<sup>1</sup>

In a recent and excellent survey of graphene electrodes by Jo et al. (2012), the solution based methods are estimated to give sheet resistances at least an order of magnitude higher than are available in electrodes made by CVD (chemical vapor deposition). In the spectrum of applications it seems clear that the lower cost of the solution-based methods will be the dominant factor in many cases. We return to this topic at the end of [Chap. 3](#).

## 2.2 Direct Spontaneous Synthesis of Crystalline Graphene in Plasma and in Solution

While it has been said that graphene crystals cannot be directly grown (the restriction applies to indefinitely large crystals), spontaneous crystallizations of graphene have been demonstrated by Dato et al. (2008), Choucair et al. (2008), Lin

<sup>1</sup> There is a possibility that introducing one of the intercalant metals like K (e.g., by heating the sample in K vapor in a closed cell) during or after the spin-coating step might substantially improve the conductivity. These platelets are so refractory that simple heating does not improve their electrical contact.).

et al. (2011a), Deng et al. (2011) and Singh et al. (2011). The first report, of Dato et al., involved spraying ethanol droplets into an Ar plasma, with the results of rapid crystallization being caught on nylon membrane filters. Single layer graphene was clearly identified, along with bilayer and several-layer graphenes. The potential for large scale production is noted, with 2 mg/min of carbon being obtained for an input of 164 mg/min of ethanol.

The four following demonstrations are of spontaneous crystallizations from liquid solution, in sealed autoclave vessels, in reactions described as “solvothermal synthesis”. These methods are straightforward chemistry, combining a carbon source like  $\text{CCl}_4$  with K or Na metal to give free carbon and NaCl or KCl. The three papers mentioned use similar processes, and we describe the work of Lin et al. (2011a) as exemplary in the quality of the graphene obtained, and also in the clarity in which the method and favorable results were presented, rather closely following the earlier work of Choucair et al. The new method, that can be described as a “one pot process”, is capable of bulk production of single and several layer graphene, including chemical substitutional doping of boron and nitrogen.

In what seems the clearest example, facile growth from solution of both pure- and boron-doped graphene crystals has recently been demonstrated by Lin et al. (2011a). These authors demonstrate that these graphenes form rapidly from nascent carbon and boron in reduction reactions of  $\text{CCl}_4$  and boron tribromide ( $\text{BBr}_3$ ) using alkali metal K as reductant. The products of the solution reaction appear to be free crystalline flakes of graphene and boron doped graphene, plus KCl and KBr. In a beautifully simple process to make boron-doped graphene, the authors place, into a Teflon-coated stainless steel autoclave of capacity 50 ml: 10 ml of  $\text{CCl}_4$ , 50  $\mu\text{L}$   $\text{BBr}_3$  and 1 g of potassium K. The autoclave is sealed and heated at 160 °C for 20 h, and allowed to cool. The resultant product was dispersed in acetone under stirring to remove  $\text{CCl}_4$  from the products. After filtering, the remaining product was washed with deionized water (1 L). The suspension was vacuum filtered and dried in a vacuum oven at 100 °C for 12 h. (The method is almost exactly that of Choucair et al. 2008, the pioneering work.) The yield of graphene was observed to be about 0.4 g C per gram of K, in both the pure and boron doped cases. This remarkable work demonstrated single layer sheets of graphene of lateral extent exceeding five micrometers, after sonication of the product described above for 40 min in ethanol. It was estimated that 13.6 % of the flakes resulting were single layer graphene. An Atomic Force Microscope (AFM) image (15 × 15  $\mu\text{m}$ ) in their Fig. 1d shows a 0.7 nm vertical step (indicating a single layer of graphene) at the edge of a sheet extending at least 5  $\mu\text{m}$ . This process of spontaneous growth of micrometer scale single and few-layer plates of graphene in solution (without deliberate nucleation sites) is perhaps a solution analog, of the CVD process of growing carbon nanotubes using nanometer size Fe particles as catalysts. The authors use Raman spectra and measurements of the 1s XPS spectra of boron and carbon to establish that in their products the B and C atoms are in  $\text{sp}^2$  trigonal planar bonds expected in graphene. The authors establish that the conductivity of their graphene is higher than that of reduced graphite oxide flakes that they prepared for comparison.

Singh et al. (2011) confirm a solvothermal process using ethyl alcohol as carbon source in a medium pressure autoclave. In their process at about 230 °C they note a pressure of about 60 atmospheres, leading to graphene sheets from monolayer to trilayer thickness. They use sodium borohydride as a reducing agent instead of sodium metal. They note that their process is similar to a chemical process for making carbon nanotubes as described by Wang et al. (2005).

Recently, Deng et al. (2011) grow nitrogen-doped graphene in similar reactions using an autoclave with nitrogen: for example, by reacting 20 mL of  $\text{CCl}_4$  and 1 gram of  $\text{Li}_3\text{N}$  (a solid that melts at 813 °C) at 250 °C for 10 h. The product was washed sequentially with 18 wt % HCl, water, and ethanol, and then dried at 120 °C for 12 h. The authors state that in each batch with a 40 mL autoclave they produce about 1.2 g of carbon product. The N doping of the product was measured by XPS to be between 4.5 and 16.4 % (the latter from an augmented reaction including cyanuric chloride  $(\text{NCCl})_3$  in addition to  $\text{CCl}_4$  and  $\text{Li}_3\text{N}$ ). It appears that some of the N is not fully substitutionally bonded into the graphene, because a heating at 600 °C of the first-described product reduced its N doping from 4.5 to 3 %. In fact XPS analysis indicated two other types of N bonding, termed pyridinic and pyrrolic, in addition to the dominant graphitic bonding, in which N simply replaces C in sixfold rings. The electrical conductivity of their (heavily doped n-type) graphenes were estimated by Deng et al. (2011), using a four-point probe method, to be 0.18  $\Omega$  cm (0.15  $\Omega$  cm for the augmented preparation, with more N) compared with  $\sim 0.1$   $\Omega$  cm obtained by Schniepp et al. 2006, for reduced graphite oxide platelets.

Returning to directly precipitated graphene, it appears that the N-doped case (Deng et al. 2011) is more complicated than the B-doped case, reported by Lin et al. (2011a), where it appears that all of the B simply replaces C in the hexagonal ring structures.

It appears that these solution-grown crystals of graphene are of higher quality than platelets obtained by any of the chemical oxidation–reduction exfoliation methods applied to graphite. It is clear that the method can be scaled to large volume. These methods seem to be promising and under-utilized.

### **2.3 Comparison of Chemical Graphenes to Carbon Black, Activated Carbon and Carbon Fiber**

This book is concerned with applications of graphene, a material which, as we have seen in the above sections on chemical exfoliations, can appear as single to few-monolayer platelets whose lateral extent may be 100s of nanometers, as mentioned by Schniepp et al. (2006), and in the range 200–500 nm as evident in Fig. 1 of Stankovich et al. (2007). As suggested above, these lateral sizes are small compared to those available in the direct chemical growths, as exemplified by Fig. 1d of Lin et al. (2011a). Although Segal (2009) suggests that graphenes such

as those obtained by Stankovich et al. (2007) and Schniepp et al. (2006) were produced in volumes 15 tons/year in 2009, with anticipated increases, these volumes are small compared to volumes of well-established commercial pure carbon products “carbon black”, “activated carbon”, and “carbon fiber”, for which applications to some degree overlap.

These three products are based on graphitic carbon, as indicated by their relatively high electrical conductivity and black color. True amorphous carbon is a wide band gap semiconductor, insulating and non-absorbing of light. It appears that the nanocrystalline core of carbon black is on the scale of 2 nm, that of activated carbon perhaps 20 nm, while carbon fiber is made of long linear filaments bound together into long ropes or cylinders. These products vary in detail as developed for particular applications.

An exemplary form of conductive “carbon black”, commercial product Cabot XC-72, was described by Muller et al. (1999) as amorphous with particle size 2 nm and surface area 250 m<sup>2</sup>/g. Carbon black, density in the range 1.8–2.1 g/cc, is said to be produced in volume  $8 \times 10^6$  tons per year, by incomplete combustion of various heavy petroleum products, called tars. Approximately 70 % of carbon black used as a reinforcing phase in automobile tires, where it facilitates heat conduction, and as a pigment. A resistivity of 0.08  $\Omega$  cm is given for XC-72 commercial carbon black, and for commercial carbon black (Alpha Aesar) a value of 1.0  $\Omega$  cm. According to Muller et al. (1999), the XC-72 carbon black of Cabot Corp. has particle size about 2 nm and surface area 250 m<sup>2</sup>/g. A nominally similar product, Akzo Nobel EC-600JD is found by Muller et al. (1999) to have surface area 1,300 m<sup>2</sup>/g.

As suggested above, experimental measurements show that pure amorphous carbon (“amorphous diamond”), is a wide bandgap semiconductor with tetrahedral sp<sup>3</sup> bonding, at density 2.9 g/cc, a density much higher than graphite but less than diamond, 3.5 g/cc. See for example McKenzie et al. (1991), their Fig. 7, a plot of the radial distribution function G(r) for undoped vacuum-arc-deposited carbon, that resembles the G(r) computed for liquid carbon. The resistivity reported by these authors, 10<sup>7</sup>  $\Omega$  cm is much higher than for the commercial products. So it appears that commercial carbon black, some referred to as conductive blacks, is quite different from pure amorphous carbon, that is well defined and well understood in careful laboratory work with matching theoretical treatment.

A second major pure carbon product is “activated carbon”, sometimes referred to as AC, that is primarily derived from coal, peat, or nut shells at a volume perhaps 2 million metric tons per year. According to Muller et al. 1999 “activated carbon” has a higher surface area, in the range 500–1,500 m<sup>2</sup>/g (compared to completely exfoliated graphite, 2,630 m<sup>2</sup>/g) and has widespread use for sorbing undesired chemicals as in water purification, air purification and as an antidote for swallowed poison.

A careful TEM study (Harris et al. 2008) of an exemplary activated carbon, Norit GSX powder, derived from peat (a recent biological residue) found that the particles of porous powder were disordered, but composed mostly of tightly curled

single carbon layers with pore size about 3 nm. Harris et al. (2008) describe Norit GSX, also described as activated charcoal, as produced from peat, carbonized in inert atmosphere at 500 °C, followed by activation by heating in steam at 1,000 °C, and washing in HCl. Norit GSX has a surface area, according to Harris et al. (2008), of 950 m<sup>2</sup>/g. According to Gamby et al. (2001), Norit activated carbon (AC) powder has a surface area 1,200 m<sup>2</sup>/g and resistivity 3 Ω cm. (It is tempting to attribute this higher resistivity, compared to the ~0.1 Ω cm of the reduced graphite oxide reported by Schniepp et al. 2006, to the smaller lateral extent of the graphitic planes, ~20 nm in activated carbon to the 200–500 nm of lateral extent in the exfoliated products.) Gamby et al. (2001) found that a similar powder, PICTACTIF SC carbon, had a specific capacitance of 125 F/g, which is of interest for supercapacitor application (to be discussed in [Chap. 3](#)).

Activated carbon is obtained from sources that are described as “non-graphitizing” (Franklin 1951), meaning that they cannot be turned entirely into six-fold bonded carbon even by heating to 3,000 °C. Harris et al. take the position, perhaps somewhat controversial, that the non-graphitizing form of activated carbon includes 5-fold rings (as do the curved fullerenes) that, once formed, cannot be removed. Harris et al. suggest that the 5-fold rings account for the curvature of the single carbon sheets seen in their TEM image of Norit GSX, and correlate with the high surface area.

“Carbon fiber”, the additive for a major contemporary structural material, the “carbon fiber composite”, is composed of larger strands of graphitized carbon 6–10 μm in diameter, produced either from petroleum pitch or from polyacrylonitrile (rayon), where the stacking of parallel layers is turbostratic (random) rather than of the Bernal AB type in the petroleum pitch products. Carbon fiber-reinforced polymers are important in light-weight structural materials, used, for example in helicopters, jet aircraft and bicycle frames, where light weight, strength and flexibility are important. An estimate of the market for carbon fiber composites in 2009 is \$11 B. Use of carbon fiber in expensive automobiles is described by Brown (2013), who points out that the cost in this application is mostly in the processing, explained in some detail, rather than in the raw material. Only a small part of the carbon fiber market seems susceptible to graphene as an alternative, but Head, manufacturer of expensive tennis racquets as well as of expensive skis, has announced new racquets that incorporate, in their words, “the world’s strongest and lightest material”.

These small particle forms of carbon, apart from activated carbon, are used as fillers in a range of applications. Carbon black is used in tires, in nanocomposites to impart strength and electrical conductivity, and may be incorporated in the skin of stealth aircraft to absorb radar pulses. Compared to carbon black, it seems that the larger platelets of graphene will be more expensive to produce and may likely only find reasonable application where the higher electrical conductivity is important. The traditional forms of small particle carbon, carbon black, activated carbon and carbon fiber, with large volumes and low commodity prices, are not suitable for transparent electrodes, nor for electronic logic, where the need for plate geometries with high aspect ratio clearly leaves open new applications for

graphene. It remains to be seen whether the small platelets of graphene will form adequate electrodes for solar cell and other electrode applications. An important issue is the electrical connectivity between platelets, that may not suffice for some electrode applications, although it may suffice for electromagnetic shielding applications.

Higher level electronic applications can be addressed by large area continuous polycrystalline graphene, that can now be made by chemical vapor deposition, CVD.

## 2.4 Chemical Vapor Deposition-Based Methods CVD

It has been known for some time that graphene growth from carbon-containing gases can be catalyzed by various transition metal substrates. This can be described as catalytic cracking of a hydrocarbon source such as methane or acetylene, or precipitation of dissolved carbon (perhaps from a cracking process) onto a metal surface with subsequent graphitization (ordering into the hexagonal lattice). Reports include Grant and Haas (1970); Gall et al. (1987); Nagashima et al. (1993); Gall et al. (1997); Forbeaux et al. (1998); Affoune et al. (2001); Harigaya and Enoki (2002). Limited solubility of C in the substrate can restrict the production to single layers of graphene, a desirable outcome.

An important discovery of Reina et al. (2008) was that single crystal (and, later, also continuous polycrystalline CVD) graphene could be released from the traditional oxidized silicon substrate to be relocated to a different target substrate.

The steps used by Reina et al. (2008) include covering (spin-coating) the film with poly(methyl methacrylate) (PMMA, 950,000 molecular weight, 9–6 wt % in anisole), followed by partially etching the surface of the SiO<sub>2</sub> in 1 M NaOH aqueous solution. The 300 nm SiO<sub>2</sub> does not etch completely, and only a minor etching is enough to release the PMMA/graphene layer from the silicon. The release is typically accomplished by placing the substrate in water at room temperature, where manual peeling can be used to detach the PMMA/graphene membrane from the substrate. As a result, a PMMA membrane is released with all the graphite/graphene sheets attached to it. This membrane is laid over the target substrate, and the PMMA is dissolved carefully with slow acetone flow. The flakes in the original work of Reina et al. (2008) are on the micrometer scale, obtained from micromechanically cleaved graphite.

This basic transfer technique was quickly adapted to much larger area graphene films grown by chemical vapor deposition CVD on transition metals, principally Ni and Cu.

Li et al. (2009) extended this basic method of growing graphene on copper foil, followed by transfer using the Reina method, to the centimeter scale, transferred to a Si substrate. Li et al. (2009) use chemical vapor deposition with methane as the carbon source, flowing over copper foil about 25 μm in thickness at temperatures up to 1,000 °C. It was found that the growth was complete in 30 min, and was

self-limiting, so that only 5 % of the area had more than one layer of graphene. The graphene was found to be continuous, growing across lattice defects in the copper substrate. The mobility in the grown films was measured as high as  $0.4 \text{ m}^2/\text{Vs}$ . The films were transferred to arbitrary substrates by a method similar to that of Reina et al. (2008).

Reina et al. (2009) also extended their method (Reina et al. 2008) to growing graphene on Ni, but it now appears that Cu is more suitable for this purpose. Reina et al. (2009) include references to earlier reports of growth of graphene monolayers on single crystalline transition metals, including Co, Pt, Ir, as well as Ru, Ni, and Cu.

Large  $4 \times 4 \text{ in.}^2$  graphene films grown on copper and transferred to oxidized silicon were reported by Cao et al. (2010). They found carrier mobility about  $0.3 \text{ m}^2/\text{Vs}$  and observed both the quantum Hall effect and weak localization in measurements of the graphene.

A similar method based on Ni substrates has been described by Kim et al. (2009). These workers have produced patterned graphene by patterning a Ni deposit on a Silicon wafer ahead of the CVD growth of graphene. They also described several methods of transferring the Ni grown graphene to other substrates. Growth on Co has recently been presented by Ramon et al. (2011).

Plasma-enhanced CVD (PECVD) has been applied to growth of carbon nanostructures by several authors (Zhao et al. 2006; Wang et al. 2004; Kobayashi et al. 2007 and Chuang et al. 2007). It is not clear if the plasma-assisted aspect could be applied in the wide area growth of graphene on Cu or Ni, to allow a lower temperature deposition that clearly would be desirable.

The state of the art in growing and transferring large area graphene films is reported by Bae et al. (2010), a consortium of workers in South Korea. Bae et al. have achieved deposition on a roll of Cu foil with dimension up to 30 in. in the diagonal direction. The Cu foil is wrapped onto a cylindrical quartz substrate in the CVD reactor, so that a larger graphene area can be obtained within a tube reactor. The copper foil was wrapped around a 7.5 in. diameter quartz tube, inserted into an 8-inch-diameter quartz reactor tube of length 39 in. Adopting this geometry minimized temperature gradients over the copper area, to promote homogeneity of the deposited carbon. The authors describe a preliminary step of annealing the copper foil in flowing  $\text{H}_2$  at  $1,000 \text{ }^\circ\text{C}$  to increase the grain size of the Cu from a few  $\mu\text{m}$  to around  $100 \mu\text{m}$ . After this annealing, methane is added to the gas flow for 30 min at 460 mTorr at flow rates 24 and 8 standard cc per minute, respectively, for methane and hydrogen. After this the furnace is quickly cooled to room temperature at  $10 \text{ }^\circ\text{C/s}$  in flowing hydrogen at 90 mTorr.

The graphene-coated large area copper foil, after removal from the quartz tube, is attached to a “thermal release tape”, a large-area thin polymer supporting sheet, by running the pair of sheets between soft rollers at a pressure  $\sim 2 \text{ MPa}$ . The result, a large-area, “release tape” polymer/graphene/copper sheet sandwich is then rolled through a chemical bath to remove the copper. The next step is to place the graphene side of the assembled sheet onto the substrate of final choice, that is often a roll of  $188 \mu\text{m}$  thick polyethylene terephthalate (PET). Running this

sandwich between rollers at mild heat  $\sim 100$  °C transfers the graphene from the “thermal release tape” to the desired final support. In typical cases the procedure is iterated to give a stack of four graphene layers (whose azimuthal orientations are random) on the wide area PET supporting sheet, and with diagonal dimension as large as 30 in. This stack is a high quality transparent flexible conductor at best with  $\sim 90$  % optical transmission and low resistance of  $\sim 30$   $\Omega$ /square. This low value was aided by a step of “chemical doping” with nitric acid  $\text{HNO}_3$ , that makes the films strongly p-type. According to the authors, Bae et al. (2010), this transparent conductor is superior to common transparent conductors such as Indium tin oxide (ITO) and carbon-nanotube films, reported by Lee et al. (2008). Bae et al. (2010) describe steps in producing touch screens for electronic devices using their graphene/PET transparent electrodes. The resulting transparent conductors display extraordinary flexibility, and it was stated that the electrode functions up to 6 % strain.

Aspects of the growth of graphene on Cu that may be improved are the high temperature, 1,000 °C, conventionally needed, the rather small size of the polycrystalline graphene grains typically resulting, and, of course, the problem of removing the copper from the graphene.

To begin, note that the interaction of carbon with copper is much weaker than with carbon (differing from Ru, where epitaxy of C is achieved, with corrugations of the graphene to match the lattice). The Cu does nucleate islands of graphene, but without strong relations between the axis directions in the graphene and the copper.

The growth of graphene on Cu foil, typically of (100) surface orientation, is successful, but leads to lower mobility than that of micromechanically cleaved graphene. Intuitively it seems that grain boundaries are likely the cause of lower mobility, although it may be affected by lack of cleaning of adsorbates or stray electric fields from the support of the graphene during the measurements. A theoretical discussion of growth on Cu (111) has been given by Chen et al. (2012) that seems useful even though the copper foils in use have (100) surface orientations.

Li et al. (2011a) report growing “single crystals” of graphene on Cu (100), of 0.5 mm size, remarkably large indeed, and larger than grains in the underlying Cu. They comment that the employed foil displayed “a highly faceted, rough Cu (100) surface with sharp diffraction spots”. They also comment that the diffraction pattern of the graphene looked like that of free standing graphene, “perhaps indicating a weak coupling to the rough surface”. In fact the mobility in their “single crystals” was  $0.4 \text{ m}^2/\text{Vs}$ , very high, but not a single crystal value as obtained on free cleaned graphene. A method of growing oriented single crystal graphene on Cu without grain boundaries would be an important advance. Chen et al. (2012), presuming Cu (111), note that this surface has hexagonal symmetry matching the graphene benzene ring symmetry. (Cu 111 may be easily available, as it results from evaporation of Cu, as shown by Tao et al. (2012), allowing in CVD growth also excellent monolayer graphene.) On Cu (111), however, Chen et al. find in simulation that a typical nucleated seven-ring cluster (a ring surrounded by six rings, this resembles the coronene molecule), initially benefitting

from the common hexagonal shape, in fact reduces its energy by rotating  $11^\circ$  relative to the hexagon of the underlying Cu. For this reason Chen et al. (2012) argue that orientational disorders of carbon islands will be abundant in the early stages of nucleation and growth on Cu (111). Such disorders cannot heal with the enlargement of the islands, leading to the prevalence of graphene grain boundaries upon island coalescence. Chen et al. go on to suggest that by adding Mn to the Cu, a Mn-Cu (111) surface of hexagonal symmetry could easily be obtained that would exactly stabilize the common “coronene” seven-ring precursor. They in fact suggest that molecular coronene vapor be used in a two-stage CVD process (it has been shown by Li et al. (2011b) that benzene, when used in the CVD process on Cu, allows graphene growth at  $300^\circ\text{C}$ , much lower than the typical  $1,000^\circ\text{C}$ ). The suggested coronene deposition, followed by de-hydrogenation, would leave a network of like-oriented graphene nuclei that would then be filled in, in a second stage, by CVD of methane or ethylene in the usual way. In this two stage growth, on a modified Cu (111) surface, it appears that grain boundaries would not arise and a graphene single crystal could be envisioned of very large lateral size and controlled orientation, as suggested by Chen et al. (2012). As noted above, Li et al. (2011a) have already reported growing single crystals as large as 0.5 mm, on Cu, but without control of the orientation of the graphene.

These reports are promising regarding the chance of larger grain size and also lower deposition temperature for graphene grown on copper.

The problem remains that Cu is not a useful substrate in most cases. It would be helpful to find ways to grow graphene on silicon, for example. A preliminary report of UHV growth of graphitic carbon directly onto Si (111) by e-beam deposition was given by Hackley et al. (2009). The silicon surface temperature was initially  $560^\circ\text{C}$ , leading to a thin amorphous carbon layer, and then raised to  $830^\circ\text{C}$  where graphitic carbon was observed to grow. The grain size of graphitic carbon was in the one nanometer range in this report, which is not very promising.

An interesting chemical approach to growing reproducible graphene nanoribbons has been described by Koch et al. (2012). These workers fabricated long narrow armchair graphene nanoribbons on a gold surface, Au (111). The processing was done in ultrahigh vacuum (UHV), evaporating the 10,10'-dibromo-9,9'-bianthryl (DBDA) precursor molecules from a Knudsen cell at 470 K. The word “bianthryl” indicates a molecule composed of two anthracene molecules, and anthracene in turn is three benzene rings in a row. These molecules polymerize in a linear fashion on the Au surface, to lead, finally, to chemically-synthesized nanoribbons with perfect armchair edges. Thus, the ribbons alternate between two- and three- benzene rings in width. Koch et al. used STM to study the “voltage-dependent conductance” as single ribbons are pulled free of the gold surface. While the authors do not describe the nanoribbons as metallic, they did observe currents up to 100 nA through these structures. The large current density suggests that the nanoribbons support metallic conduction in a 1D band above a band-edge energy. The ribbons were mechanically robust and were moved around the gold surface using the STM tip. The methods are attractive in achieving long ribbons of precise width and edge structure, and also in that the highest temperature in the

fabrication is only 400 °C. Producing wider ribbons and also finding ways to locate the ribbons where they are needed are issues facing application of this method.

## 2.5 Silicon Carbide Epitaxial Growth

Graphene with long range order can be obtained by heating SiC single crystals in vacuum. Wafers of SiC are commercially available, and form the basis for graphene transistor fabrication. Silicon carbide can be viewed as a layer compound, composed of polar SiC layers. The bonding in SiC is principally covalent, as in diamond C and in Si, but the elemental difference imparts some ionic character. The polar tetrahedrally-bonded layers of importance are arranged perpendicular to the  $c(0001)$  direction. There are two types of stacking of the SiC layers, cubic stacking and hexagonal stacking. The important hexagonal “polytypes” 4H and 6H, comprise, respectively, 4 and 6 such hexagonally stacked bilayers per unit cell. In 4H-SiC and in 6H-SiC the Silicon polar surface is designated “0001” while the polar Carbon surface is designated  $[000(-1)]$ . All of these crystals are insulators, with bandgaps 3.02 eV for 6H-SiC and 3.27 eV for 4H-SiC. (Seyller 2012). Graphene layers can be epitaxially formed by heating SiC in vacuum, as Si atoms leave and the surface reconstructs. A detailed procedure has evolved using the silicon face SiC(0001).

Growth of graphene by heating these surfaces was first demonstrated by Van Bommel et al. (1975), and confirmed by Forbeaux et al. (1998), who show 6-fold LEED pattern of crystalline graphite after annealing 6H-SiC(0001) surface at 1,400 °C, observed with primary energy 130 eV, The growth methods were recently reviewed comprehensively by Seyller (2012). An earlier review of growing graphene and bilayer graphene on SiC was given by Bostwick et al. (2009), who also make extensive use of the surface technique angle resolved photoemission spectroscopy (ARPES).

The electronic band structure of graphene grown on SiC has been investigated and found to be nearly ideal by Sprinkle et al. (2009). Their methods include ARPES and surface X-ray diffraction (SXRD). Studies of graphene grown on SiC have revealed that even multi-layer growths retain single layer electronic properties (Hass et al. 2008). It is generally found that graphene on SiC is conductive with electrons, an n-type film with Fermi energy in the order of 0.3 eV.

While the SiC crystalline substrate imparts long range order to the grown graphene, the resistivity of the grown layers is not as low as obtained in flakes micro-mechanically exfoliated from graphite. A leading cause of this degradation appears to be steps on the SiC face, whose effect on the resistance of epitaxially grown single layer graphene was investigated by Ji et al. (2012). The effect of the steps is apparently not to disrupt the order of the grown graphene but to cause jumps in the doping level.

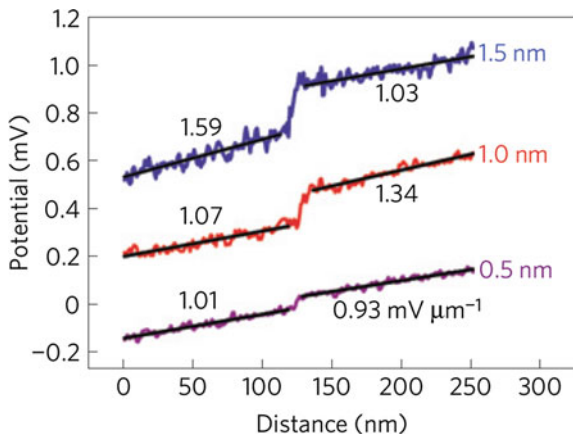


**Fig. 2.3** Scanning tunneling potentiometry measurements on single layer graphene on SiC in traces (*top to bottom*) crossing steps of heights 1.5, 1.0 and 0.5 nm, respectively. The numbers shown close to the data traces indicate the slopes in mV/μm on the terrace before and after the step is encountered. The authors confirmed that the voltage drops across the steps scale with the injected current. (Reprinted figure with permission from Ji et al., Fig. 3c. Copyright (2012) by Nature Materials)

The Scanning Tunneling Potentiometer device of Ji et al. (based on that of Bonnani et al. (2008), see also Homoth et al. (2009)) deploys three tips: two are current-injecting probes in contact with the surface, typically separated by  $\sim 500 \mu\text{m}$ , and the third is a scanning tip. Data from this method is given in Fig. 2.3.

The scanning tip measures the topography as well as the local potential, as affected by the imposed current flow. The parameter values relevant to the Fig. 2.3 are temperature 72 K, voltage drop between current injecting tips 1.53 V, the estimated local current density in the single monolayer graphene layer in the measured region,  $6.4 \times 10^{-6} \text{ A}/\mu\text{m}$ . The carrier density in the graphene is estimated as  $10^{13} \text{ cm}^{-2}$ , and the mobility is estimated as  $0.3 \text{ m}^2/\text{Vs}$ .

The authors find that voltage-drops across steps contribute significantly to the total drop across a sample. A 0.5 nm substrate step contributes extra resistance equivalent to a terrace about  $\sim 40 \text{ nm}$  wide, while 1.0 and 1.5 nm high steps contribute resistances, respectively, equivalent to terraces  $\sim 80 \text{ nm}$  wide and  $\sim 120 \text{ nm}$  wide.

Realistic calculations of the extra electrical resistance that appears when graphene “flows” over a step of height  $h_s$  on a SiC substrate, have been carried out by Low et al. (2012), as suggested in Fig. 2.4. (This situation occurs in device applications as reported by Lin et al. (2010), to be discussed in Chap. 5, see Fig. 5.1. More work on related step-geometries has been carried out by Sprinkle et al. (2010) and by Hicks et al. (2012), to be described in Chap. 4.) Referring to Fig. 2.4, the “step-resistance effect”, as interpreted by Low et al. (2012), will vary according to the degree to which the substrate in question changes the carrier

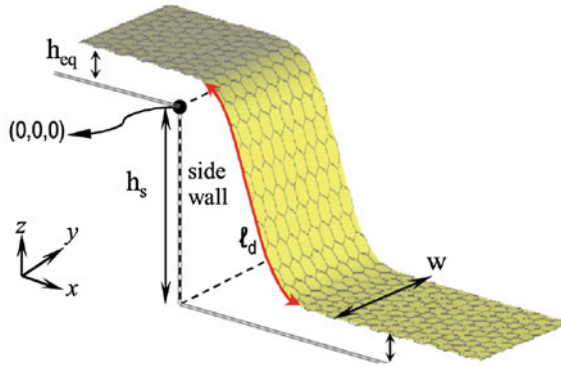


**Fig. 2.4** A large incremental resistance is measured when graphene “flows” over a step-edge on SiC, as illustrated here. The effect comes from the large difference in local Fermi level in the bound and free sections of the graphene and, according to Low et al. (2012), is not influenced strongly by the curvature. (Reprinted figure with permission from Low et al., Fig. 1. Copyright (2012) by the American Physical Society)

density of the graphene, as well as the density of steps on the substrate. (Hicks et al. (2012) have patterned deeper trenches into SiC, where they believe the graphene (subsequently grown by sublimation heating) on the trench wall, analogous to the “flowing” graphene section in Fig. 2.4, actually develops a bandgap on the order of 0.5 eV. These authors find that a locally observed energy gap is confined to regions of sharp curvature in the graphene.) The equilibrium graphene spacing from the SiC substrate is taken as 0.34 nm, with an estimate of 0.04 eV per atom binding by van der Waals interaction (Zacharia, et al. 2004).

To summarize, a lower graphene electron mobility for epitaxial films on SiC compared to mechanically exfoliated graphene placed on oxidized Si, has been connected to the presence of steps on the SiC surface. But the calculations carefully performed by Low et al. suggest that the sharp curvature suggested in Fig. 2.4, as the film flows over the step-edge, is not the source of much scattering. Rather, the extra scattering, is due to the electrical coupling between the graphene and the substrate, that varies sharply in the vicinity of the step. The authors conclude that the morphology affects the resistivity through the tendency of the SiC to dope the graphene, an effect stronger on SiC than on oxidized Si.

Adapting the SiC graphene process toward a production method, Emtsev et al. (2009) have shown that it can be carried out at atmospheric pressure, producing wafer-size layers with good results. De Heer et al. (2010) (and references therein) have demonstrated an improved form of epitaxial graphene growth: “confinement-controlled-sublimation”, including methods to produce step-free surfaces on SiC.

A useful summary of synthesis methods for graphene with emphasis on patent applications filed has been given by Samba Sivudu and Mahajan (2012). A summary of this report was given on the nanowerk website dated June 28, 2012, <http://www.nanowerk.com/spotlight/spotid=25744.php>

The patent survey suggests that large companies (Samsung leading with 16 patent applications) focus on CVD methods (92 patent applications total) suitable for electronics, while small companies (see also Segal 2009) including Angstrom Materials, XG Sciences, Vorbeck Materials Corp, focus on exfoliation methods for small platelets (94 patent applications total). This report suggests that nanoribbon manufacture based on unzipping carbon nanotubes is a synthesis method of “moderate scalability, high yield and high quality and potentially low cost” with potential applications in field effect transistors, interconnects, nanoelectromechanical devices and composites. This surprisingly positive latter assessment may build from the rather large present production of carbon nanotubes. According to Segal (2009), large chemical companies including Bayer and Showa Denko produced in 2009 100s of tons of nanotubes per year, with plans at that time to increase production to thousands of tons.



<http://www.springer.com/978-3-319-03945-9>

Applications of Graphene

An Overview

Wolf, E.L.

2014, VII, 84 p. 31 illus., 4 illus. in color., Softcover

ISBN: 978-3-319-03945-9